Heterogeneous & Homogeneous & Bio- & Nano-

CHEMCATCHEM

CATALYSIS

Accepted Article

Title: Au-Pd selectivity-switchable alcohol-oxidation catalyst: controlling the duality of the mechanism using a multivariate approach

Authors: Itaciara E. M. da S. Melo, Samuel A. A. de Sousa, Laíse N. dos S. Pereira, Jefferson M. Oliveira, Karla P. R. Castro, Jean C. S. Costa, Edmilson M. de Moura, Carla V. R. de Moura, and Marco Aurelio Suller Garcia

To be cited as: *ChemCatChem* 10.1002/cctc.201900512

Link to VoR: http://dx.doi.org/10.1002/cctc.201900512

A Journal of

ChemPubSoc Europe

WILEY-VCH

www.chemcatchem.org

10.1002/cctc.201900512

Au-Pd selectivity-switchable alcohol-oxidation catalyst: controlling the duality of the mechanism using a multivariate approach

Ms. Itaciara E. M. da S. Melo, Dr. Samuel A. A. de Sousa, Ms. Laíse N. dos S. Pereira, Jefferson M. Oliveira, Karla P. R. Castro, Dr. Jean C. S. Costa, Dr. Edmilson M. de Moura, Dr. Carla V. R. de Moura, Dr. Marco A. S. Garcia*

Chemistry Department, Federal University of Piauí, Campus Universitário Ministro Petrônio Portella, 64049-550 Teresina PI (Brazil)

*Corresponding author. E-mail: marcoasuller@gmail.com

10.1002/cctc.201900512

Abstract

Supported gold-palladium nanoparticles are highly selective catalysts for the oxidation of alcohols. However, little is known about how integrated reaction conditions can affect the chemoselectivity of a specific catalytic system. Herein, a novel Au-Pd selectivity-switchable catalyst supported on $SrCO_3$ is reported; and a multivariate optimization was suggested as the key process to understand the formation of the products better. The optimization approach considered temperature, pressure, time of reaction, and Au:Pd molar ratio, and settled that the temperature and Au:Pd molar ratio showed an important effect on the ester yield, while just the metal molar ratio significantly influenced the selectivity for the aldehyde. Thus, taking into consideration the experimental data and optimized conditions, we were able to efficiently switch the selectivity by just changing the pressure of the system in a benzyl alcohol oxidation reaction. Also, we proposed that the presence of O_2 implies that there are two catalytic pathways, which leads to different selectivity, allowing us to bring some mechanistic insights dealing with the duality of the mechanism. Such outcomes are based on dense experimental results and characterizations (FT-IR, Rietveld refinement, XPS, H_2-TPR, and EDS-STEM). The catalyst was also very stable, presenting activity up to 6 runs without loss of activity and selectivity, under certain reaction conditions.

Keywords: $SrCO_3$; Au-Pd nanoparticles; alcohol oxidation; factorial design

Introduction

In recent years, major research efforts have been given to the development of nanoparticles (NPs) and nanostructured materials with potential application in the chemical industry.[1] Following the discoveries of Haruta[2] and Hutchings[3] in the use of gold catalysts as environmentally benign processes, the catalysis by supported gold and gold-palladium NPs has established new methodologies for the achievement of organic transformations under milder reaction conditions,[4] such as propene epoxidation,[5] oxidation of several compounds[6] and other chemical matters.[7] In this scenario, oxidation reactions of alcohols can be highlighted since they are considered as fundamental functional-group transformations in organic synthesis due to the possibility of improving access to compounds like aldehydes, ketones, esters, and carboxylic acids.[8] However, the need for toxic stoichiometric reagents as manganese[9] and chromium[10] is a great disadvantage, which prompts the use of metal-based catalysts. For that, one of the reasons for the choice of a bimetallic system is the electronic coupling between the metals, which produces nanocrystals with improved physical-chemistry properties and, consequently, superior catalytic performances than single metals.[11] Moreover, the use of Au and Pd is interesting since they are miscible in a wide variety of compositions, easily forming Au-Pd alloys NPs.[12]

Catalytic systems are a long-standing challenge since their chemoselectivity is limited, requiring modulation of NPs or support surfaces[13], ligands,[14] changing on the reaction conditions[15] or the use of additives as external base[6f, 6g], which hampers their wide applications on more complex organic synthetic pathways and total synthesis.[16] Thus, selectivity and mechanisms are important features that need to be understood to assist catalysts enhancements for wide applications. To achieve high selectivity, the

production of by-products via consecutive and parallel reactions must be considered for the design of improved catalytic methods.[17] For that matter, benzyl alcohol is one of the most studied model molecules for selective oxidation reactions[7c, 18] since it allows simpler elemental considerations regarding reaction conditions, the nature of the catalyst, and mechanisms insights. Therefore, constant efforts have been made by researchers to address such correlations using this reaction model.

In addition to the bimetallic and substrate choices for specific studies, the support used as NPs carrier is essential because support effects and metal-support interactions can be considered selectivity-driving processes.[19] Strontium-based or -derived supports have been investigated in the literature, and their effect on the catalysis is quite motivating. Titanate nanotubes were modified with alkali and alkaline earth metal ions and supported with Au NPs for benzyl alcohol oxidation. The authors observed that the catalytic activity had a direct relationship with the basicity of the support without external base addition, suggesting a strong interaction between the support and the NPs.[20] Castro *et al.* observed a similar effect by using a mixture of $Sr(OH)_2$, $Sr(OH)_2$. H_2O, and $SrCO_3$; however, K_2CO_3 addition was essential for the catalyst stability.[6f] Considering that a catalytic process as a whole is a complex issue, an available tool for the correlation among all the variables mentioned above has been increasingly used to help researches: a multivariate analysis. Its efficiency in building models, optimize multifactor experiments, and evaluate the effects of plentiful aspects provides the possibility of gathering all the information and predict how a system response will be under certain conditions.[21]

Herein, we propose the synthesis of a catalyst comprised of Au-Pd NPs impregnated by sol-immobilization in $SrCO_3$. We have demonstrated that the combination of Au-Pd NPs over such support can provide a pronounced performance for the solvent-free oxidation of benzyl alcohol without the need for external base

addition. Moreover, the study of temperature, pressure, time of reaction, and Au:Pd molar ratio were optimized for attaining conversion and selectivity to benzaldehyde or benzyl benzoate using multivariate processes, aiming a selectivity-switchable system by only changing one reaction condition. We also performed a full characterization of the best catalyst for our proposes (Au:Pd molar ratio of 1:1.5), which associated with the experimental data, provided mechanistic insights. The stability of the catalyst was satisfactory, with six runs without loss of activity.

Experimental

Materials

All chemicals used in the experiments were of analytical grade, bought from Sigma-Aldrich, and used as received, without further purification.

Catalyst preparation

The catalyst was synthesized by using a method described elsewhere with modifications.[22] The preparation of a catalyst with Au:Pd molar ratio of 1:1.5 is described as an example: in a typical procedure, a previously prepared aqueous solution containing 7.1 mg of palladium(II) chloride (≥ 99.9%) in 10 wt.% HCl was added in a 30-mL aqueous solution containing 31.7 mg of gold(III) chloride solution ($HAuCl_4$, 99.99% trace metals basis, 30 wt.% in dilute HCl). The same procedure was used for the preparation of other Au:Pd molar ratios, changing the quantities of metal precursors. Such ratios will be further shown. After a 5-minute magnetic stirring at room

temperature, 0.6 mL of a 2.0 wt.% aqueous solution of polyvinyl alcohol (PVA, 80%) was added to the solution, and the system was further stirred for 5 min. Subsequently, a freshly prepared 0.1% sodium borohydride ($NaBH_4$, powder, ≥ 98.0%) aqueous solution was added dropwise under magnetic stirring. A 5-fold excess of $NaBH_4$ (mol/mol), related to the mol of metals, was added to the main mixture, changing its quantity for the different Au:Pd molar ratios. The solution turned darkish instantly after the $NaBH_4$ addition, but it was kept under stirring for 30 min. The catalyst support consists of commercial strontium carbonate ($SrCO_3$, ≥ 98%).

After the NPs synthesis, 500 mg of the support was added to the prepared sol and stirred for 2 h, at room temperature. Finally, the suspension was centrifuged at 2000 rpm for 2 min. The catalyst was dried in an oven at 50°C for 5 h before storage in an amber bottle. The blackish powder was designated as Au-Pd/$SrCO_3$.

Catalyst characterization

The scanning transmission electron microscopy (STEM) images of the as-prepared and spent (after the 6th run) Au-Pd/$SrCO_3$ catalysts were obtained with an FEI Tecnai G^2 F20 transmission electron microscope (Thermo Fisher Scientific, Massachusetts, EUA) operating at 200 kV with an energy dispersive spectrometer (Bruker XFlash 6130T Silicon Drift Detector). The element distribution maps were recorded using energy-dispersive X-Ray spectroscopy (EDS). Samples for microscopy were prepared by drop casting an isopropanol suspension of the materials over a grid comprised of carbon-coated copper, followed by drying under ambient conditions. The nanoparticles' size was determined by using the ImageJ software. For that, 200 particles were considered. The metal content in the catalysts (before and after usage) was

measured by Flame Atomic Absorption Spectroscopy (FAAS), using an AA-6300 Atomic Absorption Spectrophotometer (Shimadzu Corp, Kyoto, Japan). The digestion procedure of the samples was performed using concentrated nitric and hydrochloric acids in the ratio of 1:3 (HNO_3:HCl) at the heating of 115°C for 2 h. X-ray diffraction (XRD) pattern of the catalyst was recorded on an XRD-6000 diffractometer (Shimadzu Corp, Kyoto, Japan) with Cu Kα radiation (1.5418 Å), operating at 40 kV and 40 mA. Rietveld refinement of the as-prepared catalyst was performed using Rex 0.8.2 software. The X-ray photoemission spectra (XPS) were obtained with ESCA + spectrometer system equipped with an EA 125 hemispherical analyzer and XM 1000 monochromated X-ray source (Scientia Omicron, Uppsala, Sweden) in Al K (1486.7 eV). The X-ray source was used with a power of 280 W, as the spectrometer worked in a constant pass energy mode of 50 eV. The calibration of the XPS spectra for the charge accumulation was performed using C 1s peak (BE = 284.8 eV). The Fourier Transform Infrared Spectroscopy (FT-IR) spectra were acquired by using a Spectrum 100 (Perkin Elmer, Massachusetts, EUA), set to measure 32 cumulative scans at 4 cm^{-1}. The samples were prepared as KBr pellets. Temperature-programmed reduction with hydrogen (H_2-TPR) was carried out in a ChemBET-Pulsar instrument (Quantachrome Instruments, Boynton Beach, United States) equipped with a thermal conductivity detector. Typically, 0.05 g of a catalyst was dried under a He flow at 120°C for 1 h and cooled to room temperature. The H_2-TPR profiles were obtained between 50 and 1100°C in a flow of 10% H_2/N_2, with a linear temperature increasing rate of 10°C min^{-1}. The unit cell representation of $SrCO_3$ was modeled by the VESTA (version 3.4.0, JP-Minerals, Ibaraki, Japan) and Diamond (version 3.2g, Crystal Impact GbR, Bonn, Germany).

Catalytic procedure

All the experiments used the oxidation of benzyl alcohol as a model reaction. They were carried out in a glass Fisher-Porter reactor under O_2 pressure.[6g] The reactions were performed at different temperatures under different pressures on a magnetic stirrer coupled to a heating plate with temperature control. In a typical reaction, 1 mL (9.6 mmol) of benzyl alcohol and 43.5 mg of the catalyst (2.0 wt.% metal) were loaded in the glass tube. Then, the system was purged 3 times with a stream of oxygen, and filled with the gas at a pressure between 1 and 5 bar. The resulting mixture was magnetically stirred at 500 rpm at a selected reaction time and temperature, which will be specified. After the reaction, the catalyst was separated from the products by centrifugation. Then, 20 μL of the reaction solution was mixed with 1 mL of methylene chloride (CH_2Cl_2) to determine the oxidation product yields by GC. P-xylene was added to the product as an internal standard. Gas chromatography (GC) analyses were performed by using a GC-2010 Plus equipment (Shimadzu, Kyoto, Japan) using a Carbowax capillary column. The activity of the catalyst was measured by testing the conversion of the benzyl alcohol and the selectivity and yield of benzaldehyde and benzyl benzoate (also, the selectivity of benzoic acid was considered and is in shown in Table S1). The conversion of benzyl alcohol, product selectivity, and product yield were calculated as follow:

$$Conversion = \frac{Alcohol_{begin,mol} - Alcohol_{after.mol}}{Alcohol_{begin,mol}} \; x \; 100\% \qquad \text{Equation 1}$$

$$Selectivity = \frac{Product\ of\ interest_{mol}}{All\ products_{mol}} \; x \; 100\% \qquad \text{Equation 2}$$

$$Yield = Selectivity\ of\ the\ product\ of\ interest\ x\ Conversion \quad \text{Equation 3}$$

For catalyst recycling, the Au-Pd/$SrCO_3$ was washed with CH_2Cl_2 before each cycle and dried in an oven at 50°C.

Experimental design for catalyst performance

Two full factorial designs with four independent variables (2^4) were performed. Such a process was carried out to screen the statistically significant factors for the catalyst performance in the benzyl alcohol oxidation reaction, in terms of benzyl benzoate and benzaldehyde yields. The investigated variables and their levels (uncoded) were: pressure (1 and 5 bar), temperature (80 and 120°C), time of reaction (0.5 and 2.5 h) and Au:Pd molar ratio (1:0.1 and 1:1.5).

Regarding the benzyl benzoate yield, the significant factors were the temperature, the Au:Pd molar ratio, and their interaction. To obtain a suitable model for this product, experiments were performed with additional levels (temperatures: 71.7 and 128.3 °C; Au:Pd molar ratios: 1:0 and 1:1.8) maintaining all the others variables in proper levels (pressure: 5 bar and reaction time: 2.5 h), which were pointed out by the results from the 2^4 full factorial experimental design. Also, to evaluate the experimental variation for the validation of the model by Analysis of Variance (ANOVA) replicates (three) at the central point were carried out. After this step, the Response Surface Methodology (RSM) was used to reach a better visualization provided by the mathematical model. Finally, replicated experiments regarding only the Au:Pd molar ratios were performed to find the optimum value of this variable, maximizing the benzyl benzoate yield. Only the Au:Pd molar ratio was pointed out as significant for the

benzaldehyde yield; then, an optimum value for the Au:Pd molar ratio was searched to maximize the response, maintaining the other factors in proper levels (pressure: 1 bar, reaction time: 2.5 h and temperature: 120 °C). One-way ANOVA was used to evaluate the significance of the Au:Pd molar ratio on the yields, considering its levels. Table 1 summarizes all levels (coded and uncoded) of all the studied variables. The experiments were performed randomly at different days to avoid systematic errors. The statistical software used for calculations was STATISTICA® (Version 10.0, StatSoft Inc., Tulsa, USA). For statistically significant differences between means, a post hoc pairwise comparison with Tukey's test was used. Statistical significance was set at $P < 0.05$.

Results and discussion

Catalyst characterization

Our investigations started with the catalyst synthesis using a simple PVA-stabilized Au-Pd NPs preparation method, with reduction of the metals using $NaBH_4$.[22] Our approach enabled the synthesis of pre-formed NPs, which were immobilized onto the support. The choice of support was based on a previous study published by some of us.[6f] The strategy used at that moment was to prepare SrO upon the calcination of the product of the reaction between strontium nitrate and sodium hydroxide; however, a mixture of $Sr(OH)_2$, $Sr(OH)_2 . H_2O$ and $SrCO_3$ was obtained, yet it presented remarkable activity for the oxidation of benzyl alcohol. Since strontium compounds have not been fully studied in the literature as supports for gold, palladium, and gold-palladium NPs, and that SrO is not stable for our purposes, we have decided to explore the application of $SrCO_3$ as catalytic support. All the following characterizations were performed with

Au:Pd molar ratio of 1:1.5, due to experimental results presented forward. However, it is worth mentioning that all the Au:Pd molar ratios used herein were considered as the total amount of metal detected by FAAS (not just the moles of surface Au and Pd atoms).

We have used a commercial $SrCO_3$ material; however, as the immobilization step can promote some support modification, characterizations were necessary to discover the specific material identity fully. We aimed to have just one strontium phase to have specific metal-support interactions[23] with well-known compounds. To focus on our efforts on the accomplishment of having just one phase of the strontium compound, we have used some complementary techniques to guarantee the composition of the support, as well as the catalyst itself as a whole. FT-IR spectra were recorded for $SrCO_3$ and Au-Pd/$SrCO_3$ materials, which are shown in Fig. S1A. Both samples present the peaks that correspond to CO_3^{2-}: 698 (706), 857 (855), 1071, 1454 (1476), 1774 (1772) cm^{-1}, being the parenthesized values for Au-Pd/$SrCO_3$ catalyst, when it differs from the $SrCO_3$ itself.[24] Such differences can be associated with the interaction between the support defects and metal NPs, changing the energy of the $SrCO_3$ surface, causing slight shiftings.[25] The results suggest the achievement of a unique phase for the support used, which had to be confirmed.

To elucidate such feature, XRD patterns of the $SrCO_3$ containing Au-Pd NPs were recorded to analyze the specific crystal planes that comprise the sample. The diffractogram shows lines that correspond to the carbonate itself, once the low concentration of the Au-Pd NPs hampered the observation of their diffraction peaks in the XRD. The observed main diffraction peaks of the $SrCO_3$ (Fig. S1B) are positioned at 2θ angles of 25.21°, 25.89°, 29.61°, 31.51°, 34.48°, 35.09°, 36.23°, 36.60°, 41.32°, 44.05°, 45.65°, 46.7°, 47.7°, 49.98°, which correspond to the planes of (111), (021),

(002), (012), (102), (200), (112), (190), (220), (221), (041), (202), (132), (113), respectively. Such data can be attributed to the orthorhombic phase of $SrCO_3$.[24] In order to rely on the information of the phase purity and crystallinity, we have performed a Rietveld refinement. Table 2 shows the lattice parameters, unit structural volume, site occupancy and atomic positions determined from the refinement. The $SrCO_3$ phase is isostructural with a point-group symmetry D_{2h}(mmm) and lattice constants as follows: a = 5.0923(2) Å; b = 8.3893(8), c = 6.0100(9) Å. The Rietveld refinement fitted well to the experimental data, with values for the Goodness of Fit (GoF), $R_{profile}$ (R_p) and $R_{weighted\ profile}$ (R_{wp}) of 3.5075%, 0.2058%, and 0.2550%, respectively. All the results confirmed a unique phase comprised of $SrCO_3$ in an orthorhombic phase (ICSD 202793). A schematic representation of the coordination assembly of $SrCO_3$ is shown in Fig. S1C. The structure belongs to the crystal space group D_{2h}^{16}(Pmcn) with Z = 4. The FT-IR spectrum formerly shown validates the spatial group observed in the structural unit for the strontium carbonate. It should be noted that the number of observed bands for normally degenerate vibrations can also be used as an indication of the group of molecular points. [26] The structural unit of $SrCO_3$ contains four cations of Sr^{2+} and four anions of CO_3^{2-}. The linear molecule of O=C=O with the D_{1h} symmetry has four IR fundamental vibration modes (ν1 mode is IR inactive; ν2 bend, ν3 asymmetric stretch and ν4 planar bend around are located at 857, 1454 and 698 cm^{-1}, respectively, as shown in Fig. S1A).[27]

The composition of the catalyst was also investigated in details through elemental analysis studies using line scan and mapping in STEM mode. The catalysts were synthesized to have 2.0 wt.% of metal in different ratios, which were confirmed by FAAS. The elemental mapping shows NPs distributed all over the support, which is following the synthesis procedure (as shown in the spectrum image scanning in Fig.

1A). Fig. 1B-D illustrates the STEM-EDS images for the as-synthesized catalyst Au-Pd/$SrCO_3$ (1:1.5), where Au and Pd spatial distributions are almost overlapped with each other since the Au and Pd are intermixed in the Au-Pd NPs in accordance to the atomic interdiffusion presented by the material.[28] Such strong intermixing provides a large body of metals interfaces, favoring the catalytic activity of the system,[29] suggesting the formation of an alloy between the metals. The mean diameter for metal NPs was 4.55 ± 1.22 nm (Fig. S2). Also, the Sr spatial distribution is reliably uniform, as established in Fig 1D.

TPR-H_2 analyses were performed for the naked $SrCO_3$ and the support impregnated with the Au-Pd NPs (Au-Pd/$SrCO_3$). As displayed in Fig. 2A, $SrCO_3$ presented an H_2 consumption shoulder centered at 890°C and an intense H_2 peak consumption centered at 1024°C, which can be assigned to the reduction of the compound due to desorption of carbonate species[30] and reduction of carbonate to CO or, eventually, CH_4.[30b]After the immobilization of the metals, no new reduction peaks were detected, confirming that the reduction of Au and Pd species was efficient upon the $NaBH_4$ usage; however, the shifting of the reduction temperatures to lower values (814 and 1009°C) after the metal impregnation can be attributed to some sort of interaction between the metals and the support. The observation can be explained by H_2 absorption on the Pd[31] or Au-Pd[32] surfaces, which weaken the H-H bond, decreasing the H_2 activation barrier. Thus, it is more readily available for the strontium compound reduction. Such a feature is very important for catalysis reactions since strong interactions between the metals and the support usually enhance the catalytic activity of a given system.[33] In addition, electronic structure modulation by electron transfer among the metals also can be very expressive on the enhancement of a given catalytic system performance.[7d]

XPS analyses were performed to clarify the composition of the material and confirm the obtained information from the H_2-TPR analyses. The survey scan of the catalyst (Fig. S3) revealed the presence of Au, Pd, Sr, O, and C, as expected. The carbon content can be related to adventitious C and surface carbonates. Fig. 2B presents the high-resolution Au 4f with binding energies suggesting Au^0 species (Au $4f_{7/2}$, 82.9 eV; Au $4f_{5/2}$, 86.5 eV). Such values are following the literature[34] and with our designed process since a 5-fold excess of $NaBH_4$ was employed in a clear attempt to reduce the metals fully. No obvious peaks for Au^{3+} were detected, but they cannot be completely excluded. The deconvolution of the high-resolution Pd 3d XPS spectra presented (Fig. 2C) Pd^0 as the only chemical state (Pd $3d_{5/2}$, 334.8 eV; Pd $3d_{3/2}$, 340.0 eV). One may notice that any slight shift on the binding energy can be related to the chemical environment since a bimetallic system was under consideration[35] and, although not observed, a minor contribution from Pd^{2+} cannot be rejected.[36] The binding energy of 134.8 eV for Sr $3d_{1/2}$ (Fig. 2D) corresponds to $SrCO_3$, while the other two binding energies are attributed to Sr–O bonds (Sr $d_{3/2}$, 132.5 eV; Sr $d_{3/2}$, 134.0 eV).[37] The O 1s peaks tend to be broad due to the overlapping of components (Fig. 2E). The best fitting was achieved with two individual peaks at energies of 530.7 and 532.1 eV, which are assigned as C–OH and C–O–C species, respectively.[38] The C 1s peaks are characteristic of the carbonate support, corroborating to the other results presented herein (Fig. 2F). The binding energies of 284.4 and 286.3 eV are typically peaks of adventitious carbon. The energy of 288.8 eV can be associated with carbonate, while the 290.3 eV can be assigned to C 1s component for hydrocarbons.[39]

Experimental design for catalyst performance

Previous catalytic tests using the proposed material have shown that the main products observed in the oxidation reaction were benzaldehyde and benzyl benzoate, depending on the reaction conditions, with inexpressive benzoic acid content. Through a univariate approach, a screening of Au:Pd molar ratio was performed, which was used to choose the parameters for the multivariate methodology used in the proposed experimental design. At first sight, an effect on the catalyst selectivity was quite surprising since we just modulated the reaction conditions and the Au:Pd ratios, without any additive or changing on the solvent, as proposed before in the literature.[40] Then, a multivariate approach was proposed to evaluate how some previously chosen variable may affect the selectivity for the main products of benzyl alcohol oxidation for the system herein studied. The tests were performed individually for each product formation, in an attempt to deeply show how the reaction conditions would affect the reaction pathway.

Full factorial designs consisting of 16 experimental runs, based on responses of the benzyl alcohol oxidation in terms of benzyl benzoate and benzaldehyde yields, are shown in Table 3. As a matter of comparison, conversion and selectivity results are shown in Table S1. The coefficient of determination (R^2) of the model for benzyl benzoate yield was equal to 0.91, indicating that the independent variables were able to explain 91% of the variation on the dependent variable around the global mean. Among the investigated variables, the temperature and Au:Pd molar ratio showed a significant effect on the benzyl benzoate yield, as pointed out by the Pareto Chart of standardized effects in Fig. 3A. Such chart shows both the magnitude and importance of the parameters, and the horizontal dashed line corresponds to the *t* value from the student distribution, with 95% of confidence (p = 0.05), and proper degrees of freedom. The positive value of the significant effect of interaction between the temperature and Au:Pd

molar ratio indicates that the maximization of the response is obtained when both factors are simultaneously moved to higher levels.

Time of reaction and pressure showed no statistical significance on the benzyl benzoate yield, *i.e.*, their modifications between the studied levels were not able to promote a significant change in the response. However, for further investigations, as the model suggests that the yield is increased when the parameters are set in higher levels, it is reasonable to maintain the pressure at 5 bar and the reaction time at 2.5 h. In this context, a central composite design was proposed to obtain a quadratic model, relating the significant factors and the benzyl benzoate yield. For this, experiments were performed with additional levels for temperature (71.7 and 128.3 °C) and Au:Pd molar ratio (1:0 and 1:1.6), consisting of axial points and three replicates at the central point (see Table 3). The replicates at the central points provide a new level and are useful to access the experimental variation used in the validation of the quadratic model by ANOVA. The factorial part of the central composite design corresponds to the experiments #8, #7, #15 and #16 in Table 3. The additional data for the central composite design are presented in Table 4.

As can be seen in Table 4, the levels for the Au:Pd molar ratio are slightly different from $\pm\sqrt{2}$ (±1.41), which consists with the value for rotatability and orthogonality (designated as alpha or α), when the factorial part of the design is a full one, and it has two factors. An experimental design is rotatable if the variance of its estimations depends only on the distance from the central points, *i.e.*, if the precision of the estimated response is equal for all points situated on a circumference centered at the center of the design (for designs with more factors, it could be a sphere or a hypersphere). Also, for experimental designs, it can be said that two factors are orthogonal to each other when they vary independently. In other words, the factor level

settings for two factors are uncorrelated. Thus, the effects are estimated unconfounded with the other ones. However, rotatable or orthogonal criteria may not be strictly followed due to practical constraints on the design region, *i.e.*, a particular value may not be feasible, and a neighboring value may have to be chosen[41]. The set values (±1.14) correspond to the Au:Pd molar ratio equal to 1:0 and 1:1.6. These values were defined since initially the Au:Pd molar ratio of 1:0.1 was set at the level equal to -1. Thus, the code equal to $-\sqrt{2}$ would bring the new ratio to a logically impossible negative value. Therefore, the proposed experimental design, using coded levels for Au:Pd molar ratio as ±1.14, is near-rotatable and orthogonal, owing to the small difference of the value to reach the conditions of rotability and orthogonality.

The central composite design resulted in the quadratic model presented in Equation 4,

$$Y = 4.08(\pm 1.65) + 16.36(\pm 1.03)X_1 + 9.66(\pm 1.19)X_1^2 + 18.91(\pm 1.13)X_4 + 9.02(\pm 1.60)X_4^2 + 17.78(\pm 1.46)X_1X_4 \quad \text{Equation 4}$$

where Y stands for the benzyl benzoate yield, X_1 and X_4 stand for the Au:Pd molar ratio and temperature (as shown in Table 1), X_1X_4 stands for the interaction between the factors.

In Equation 4, the intervals of confidence at 95% of probability are presented between parentheses for each parameter. The quadratic model presented a coefficient of determination (R^2) and adjusted coefficient of determination (adj-R^2) of 0.96 and 0.92, respectively, indicating that the factors can explain a large part of the variation around the global mean and, also, that the model does not overfit the data set. ANOVA of the model is shown in Table 5, where the significance of the parameters is evaluated. All

parameters are significant at 95% of confidence level, with *p*-values lower than 0.05. Therefore, the variation explained by the model is significantly higher than the residual variation; *i.e.*, the regression is significant. On another hand, the quadratic model presented a small lack of fit, since the *F* value obtained was 192.3 (although close to the critical *F* value). Despite this, only slight variations were observed between predicted and experimental values, as one can see in Fig. 3B, which shows the plot for predicted *versus* experimental benzyl benzoate yields. Furthermore, it was observed that the distribution of the residuals is closely normal, as presented in the residuals plot of Fig. 3C and the normal probability plot in Fig. 3D.

Through the quadratic model, the response surface was obtained, and it is shown in Fig. 4A. The response surface shows an increase in the benzyl benzoate yields when both factors, temperature and Au-Pd molar ratio, are moved simultaneously to the higher levels. Thus, it would be reasonable to perform additional optimization around the higher levels of the factors. Nevertheless, the increasing of the temperature, linked to the pressure of 5 bar, could have damaged the glass Fisher-Porter reactor, since it is used for small-scale reactions, which was the case; however, the bottle can stand much lower pressures than that in a metal reactor. Hence, it hampered the employed higher level for such a variable. Therefore, it was possible to assess the conditions for the study considering the maintenance of 5 bar of pressure, achieving 120°C, to prevent critical issues. In this scenario, the last optimization was performed, under the mentioned conditions, evaluating the increasing of the Au:Pd molar ratio for the benzyl benzoate yield. For this, replicated experiments were performed for Au-Pd molar ratios of 1:1.5, 1:2 and 1:4. The results are shown in Table S2.

One-way ANOVA indicated that the means of the benzyl benzoate yields at the Au:Pd molar ratio levels (groups) did not present significant difference at 95%

confidence level. The calculated *F*-value was 1.30, and the *p*-value was 0.34; thus the between-level variation is statistically equal to within-level variation. Basically, there is no difference by using the catalyst in the proportion of 1:1.5 and 1:2 or 1:1.5 and 1:4. As a consequence, we decided to use the 1:1.5 molar ratio. Therefore, under the experimental range studied here, the best conditions for obtaining benzyl benzoate yields were: 5 bar of O_2, 2.5h of reaction, Au:Pd molar ratio of 1:1.5 and 120°C, ensuring integrity conditions for the system and the possible highest yield.

The full factorial designs consisting of 16 experimental runs (Table 3) for benzaldehyde yields as response showed a coefficient of determination (R^2) of 0.72, *i.e.*, the independent variables (factors) were able to explain 72% of the variation on the dependent variable around the global mean. Among the investigated variables, only the Au:Pd molar ratio showed a marginally significant effect on the benzaldehyde yield, accordingly to the Pareto Chart of standardized effects in Fig. 4B.

The positive value of the significant effect of the Au:Pd molar ratio indicates that the maximization of the response is obtained when this factor is moved to higher levels. The factors – reaction time, pressure and temperature – showed no statistical significance on the benzaldehyde yield. On the other hand, the model suggested that the yield is increased when these parameters are set in the higher, lower and higher levels, respectively. Also, through the Pareto chart in Fig. 4B, it can be seen that the time of reaction is more important than the pressure and temperature for the response.

To access the significance of the Au:Pd molar ratio on the cited yield, one-way ANOVA was performed on replicated experiments with Au:Pd molar ratios of 1:1.5, 1:2 and 1:4. As pointed out by the full factorial design, the remain variables were set as 1 bar, 2.5 h, and 120 °C. The results are shown in Table S3.

ANOVA indicated that the means of the benzaldehyde yield at the Au:Pd molar ratio levels (groups) presented significant difference at 95% confidence level. The calculated *F*-value was 40.01, and the *p*-value was 0.00034; as a result, the between-level variation is statistically different from within-level variation. Post hoc test of significant difference between means revealed that the mean of the benzaldehyde yield at the Au:Pd molar ratio of 1:1.5 was different from the other means at the Au:Pd molar ratio of 1:2 and 1:4, while these last two means are equal between them (Tukey's test, $p < 0.05$). In other words, there is no difference on choosing Au:Pd molar ratio of 1:2 or 1:4, as a condition for the production of benzaldehyde, but there is a difference on choosing Au:Pd molar ratio of 1:1.5. Consequently, the benzaldehyde yield mean was higher at Au:Pd molar ratio of 1:1.5, the chosen optimal molar ratio for benzaldehyde production. Considering the statistical analyses performed herein, the Au:Pd molar ratio of 1:1.5 is efficient in terms of reaction yield and selectivity changing by just adjusting the pressure of the system.

Mechanistic considerations

Inferences about the mechanism of benzyl alcohol oxidation into benzaldehyde and benzyl benzoate were based on the present reaction conditions used for the optimization of our catalyst. Such a system is complex since it encompasses gas, liquid (the substrate) and interaction between the NPs and the catalyst support; due to the possibility of multiple reaction pathways and some uncertainty, the observations are somehow limited. However, the dense experimental data herein presented and the theoretical background from the literature made us believe that we were able to present some insights into the reaction mechanism for the proposed catalyst.

The multivariate study enabled the analysis of the interaction among the chosen variables for the system. Considering the limitations of the glass reactor, the suggested model indicated that the significant variables for benzyl benzoate production were temperature and Au:Pd molar ratio, while just the metals molar ratio presented a significant effect on the selectivity for benzaldehyde. Thus, the optimized model indicated that maintaining unchanged all the variables of the system (120°C, 2.5h, and Au:Pd molar ratio of 1:1.5), except one (pressure), the catalyst would be classified as selectivity-switchable one. Such a feature is highly desirable once chemoselectivity is a challenge for catalytic systems. The model showed that the unique feature for a selectivity-switchable system is pressure: 1 bar is enough for the benzaldehyde obtaining; while 5 bar of O_2 pressure were proved to have the best effect on the benzyl benzoate production. Such findings were essential for mechanism comments.

Nepak and Srinivas have shown that the basicity of the support for Au-based catalysts influences the electronic properties and oxidation activity of the catalyst, and presented a strontium-modified titanate nanotube as one of the most prominent systems among alkali and alkaline earth metal ions,[42] showing the importance on the support choice. Our outcome related to the Au:Pd molar ratio of 1:1.5 is similar to the observed by Sarina et al., which found that the Au:Pd molar ratio of 1:1.86 was the optimal charge heterogeneity for the oxidation of benzyl alcohol.[43] Such difference may be explained by the study-type approach: we are performing multivariate analysis, and the cited study applies a univariate methodology, without considering the possible interaction among the variables of the system.

Blank experiments have shown that negligible activity was observed over the support itself, which confirms that the catalytic activity is due to the Au-Pd NPs, which is in accordance to the DFT studies performed by Cui *et al*.[7c] They have shown that the

electronegativity difference between Pd and Au bears electron-rich and slightly positively charged sites. Such heterogeneity is the reason for the improved catalytic activity observed for Au-Pd systems,[44] which can explain why our catalyst does not present the necessity of having additives, such as external base addition, to present remarkable performances. However, the intrinsic basicity of the support needs to be considered since it plays an important role for the catalytic performance, being the reason for the pursuing of a one-phase strontium compound from the initial synthesis of the catalyst. Our system is following the literature since the Au-Pd systems limit the formation of toluene, hindering the disproportionation pathway needed for its formation.[22] Also, by similarity with carbocation chemistry, the toluene formation is likely not to be formed under basic conditions, where O–H cleavage is expected to be preferred instead of the cleavage of the C–O bond of benzyl alcohol. Consequently, it appears feasible that the appropriate catalytic sites are located close to the edge of the metal particles where there are metal-support interactions. However, considering that high pressure favors the benzyl benzoate production and that low pressures produce benzaldehyde, we believe that the O_2 concentration may lead to different reaction mechanism for the formation of both products. It has been proposed that the differences in the selectivity for Au-Pd systems can be explained by a decrease in oxygen adsorption on their surfaces.[45]

In light of the foregoing, we can comment on the reaction mechanism based on the experimental data we have presented. Fig. 5 shows the reaction mechanism for the benzaldehyde formation, illustrating that the reaction proceeds with the synergy between the Au-Pd NPs and the basic sites on the surface of the $SrCO_3$ (**I**). In the first step, benzyl alcohol interacts with the basic site Sr^{2+} of the support (**II**), causing an abstraction of the proton by the O^- of the carbonate, which provides an alkoxide

intermediate (**III**) in the interface of the Au-Pd alloy and the surface of the support. In the second step (**IV**), we propose that the intermediate goes through coordination with the Au-Pd alloy to form an unstable metal-H bond (metal-alcoholate). This intermediate undergoes β-hydride elimination, which forms metal-hydride species and releases the product (benzaldehyde). Then, the electron-rich surface of the alloy activates the molecular oxygen and produce activated oxygen species, which removes the H from the alloy surface, producing water and oxygen as a by-product and restoring the catalyst for a new catalytic cycle (**V**).[20]

Fig. 6 shows the reaction mechanism for the benzyl benzoate formation, which applies the same idea from the previous mechanism, *i.e.*, the synergy between the Au-Pd NPs and the basic sites of the support (**I**). However, it appears that the basic sites have little impact on the selectivity once the pressure increasing led to a selectivity change. Thus, the proposed mechanism for benzyl benzoate formation involves oxygen species that are far from just an H-abstraction process, as seen in the benzaldehyde production mechanism. To start, benzyl alcohol interacts with the basic site Sr^{2+} of the support (**II**), forming an alkoxide intermediate (**III**), where the oxygen species interacting with alloy directly attacking the $–CH_2–$. Such a mechanism provides coordination of the substrate moiety with the alloy and metal-H bond formations, eliminating water. The coordinated substrate forms a carbonyloxyl intermediate (**IV**). The next step counts with the interaction of a new benzyl alcohol molecule with a neighbor basic site, producing the benzoate (**V**), and restoring the catalyst.[45]

Recycling experiments

The previous section presents the versatility of the catalysts; however, as the exploitation of the support was an important feature to be pursued, recycling experiments were proposed to evaluate the stability of the catalyst. As shown in Fig. 7, the catalyst kept the high activity in 5 runs, leading to conversions of more than 90% in just 2.5 h, using the optimized conditions for benzaldehyde formation (the results are presented in yield for benzaldehyde). The catalyst did not need base addition to keep its performance; in addition, from one cycle to the other, it was just washed with CH_2Cl_2 and dried in an oven for 2 h. This result suggests that no deactivating processes took place and that the catalyst can be used in additional runs. The yield presented maintenance as well, which could be switched to benzoate, following the data presented before.

The elemental mapping for the spent catalyst (Fig. S4), after its 5^{th} run, presented mean diameter for metal NPs of 4.64 ± 1.42 nm (Fig. S2), i.e., no aggregation was observed when compared to the as-prepared catalyst. Also, FAAS analyses presented no metal leaching in the successive cycles. These results suggest that the catalyst can have industrial potential considering the straightforward catalyst usage.

Conclusions

Au-Pd NPs were supported effectively on $SrCO_3$. The catalysts were characterized by different techniques to guarantee the support phase composition and the oxidation of the metals. The catalytic activity of the supported catalyst was studied in the oxidation of benzyl alcohol using oxygen as oxidant under solvent-free conditions. The experimental designs suggested that the temperature and Au:Pd molar ratio were the most significant effects for the benzyl benzoate production, while just the

metal molar ratio presented significance for the selectivity of benzaldehyde. Using the optimum conditions of 120°C, 2.5 h, and Au:Pd molar ratio of 1:1.5, only the pressure was changed for a selectivity switch. The optimization methodology combined with the characterization techniques allowed some mechanisms insights, suggesting a dual mechanism depending on the O_2 pressure. The catalyst was stable and used 6 times without loss of performance.

Acknowledgments

The authors acknowledge financial support from FAPEPI, Capes, and CNPq. Thanks to CCMC/CDMF (FAPESP No. 2013/07296-2, Brazil) for the XPS measurements. The authors also acknowledge Instituto de Pesquisas Energéticas e Nucleares, IPEN-CNEN, for the TPR analyses and Dra. Liane M. Rossi for the atomic absorption analyses.

References

[1] a) W. J. Stark, P. R. Stoessel, W. Wohlleben, A. Hafner, *Chem. Soc. Rev.* **2015**, *44*, 5793-5805; b) L. M. Dias Ribeiro de Sousa Martins, S. A. C. Carabineiro, J. Wang, B. G. M. Rocha, F. J. Maldonado-Hódar, A. J. Latourrette de Oliveira Pombeiro, *ChemCatChem* **2017**, *9*, 1211-1221.

[2] M. Haruta, T. Kobayashi, H. Sano, N. Yamada, *Chem. Lett.* **1987**, *16*, 405-408.

[3] G. J. Hutchings, *J. Catal.* **1985**, *96*, 292-295.

[4] a) H. Alshammari, M. Alhumaimess, M. H. Alotaibi, A. S. Alshammari, *Journal of King Saud University-Science* **2017**, *29*, 561-566; b) C.-H. Tsai, M. Xu, P. Kunal, B. G. Trewyn, *Catal. Today* **2018**, *306*, 81-88.

[5] a) B. Dragoi, I. Mazilu, A. Chirieac, C. Ciotonea, A. Ungureanu, E. Marceau, E. Dumitriu, S. Royer, *Catal. Sci. Technol.* **2017**, *7*, 5376-5385; b) X. Feng, N. Sheng, Y. Liu, X. Chen, D. Chen, C. Yang, X. Zhou, *ACS Catal.* **2017**, *7*, 2668-2675; c) Z. Lu, M. Piernavieja-Hermida, C. H. Turner, Z. Wu, Y. Lei, *J. Phys. Chem. C* **2018**, *122*, 1688-1698.

[6] a) R. Güttel, M. Paul, F. Schüth, *Catal. Sci. Technol.* **2011**, *1*, 65-68; b) F. Kettemann, S. Witte, A. Birnbaum, B. Paul, G. Clavel, N. Pinna, K. Rademann, R. Kraehnert, J. r. Polte, *ACS Catal.* **2017**, *7*, 8247-8254; c) J. C. Costa, R. V. Gonçalves, É. Teixeira-Neto, L. M. Rossi, *ChemistrySelect* **2017**, *2*, 660-664; d) A. Teixeira-Neto, R. V. Gonçalves, C. Rodella, L. M. Rossi, E. Teixeira-Neto, *Catal. Sci. Technol.* **2017**, *7*, 1679-1689; e) G. M. Mullen, L. Zhang, E. J. Evans, T. Yan, G. Henkelman, C. B. Mullins, *PCCP* **2015**, *17*, 4730-

4738; f) P. R. Castro, A. S. Garcia, W. C de Abreu, A. A. de Sousa, V. R. de Moura, C. S. Costa, E. M de Moura, *Catalysts* **2018**, *8*, 83; g) W. C. de Abreu, M. A. Garcia, S. Nicolodi, C. V. de Moura, E. M. de Moura, *RSC Adv.* **2018**, *8*, 3903-3909.

[7] a) K. Luo, L. Zhang, H. Jiang, L. Chen, S. Zhu, *Chem. Commun.* **2018**, *54*, 1893-1896; b) S. A. Shahzad, M. A. Sajid, Z. A. Khan, D. Canseco-Gonzalez, *Synth. Commun.* **2017**, *47*, 735-755; c) W. Cui, Q. Xiao, S. Sarina, W. Ao, M. Xie, H. Zhu, Z. Bao, *Catal. Today* **2014**, *235*, 152-159; d) J. Zhao, R. Jin, *Nano Today* **2018**, *18*, 86-102.

[8] a) D. Shi, J. Liu, R. Sun, S. Ji, S. M. Rogers, B. M. Connolly, N. Dimitratos, A. E. Wheatley, *Catal. Today* **2018**, *316*, 206-213; b) D. Nepak, S. Darbha, *Catal. Commun.* **2015**, *58*, 149-153; c) Y. Zhang, F. Gao, M.-L. Fu, *Chem. Phys. Lett.* **2018**, *691*, 61-67; d) M. Khawaji, D. Chadwick, *ChemCatChem* **2017**, *9*, 4353-4363; e) R. Tan, W. Zhang, Z. Xiao, J. Wang, W. Fu, D. Yin, *ChemCatChem*.

[9] R. J. Gritter, T. J. Wallace, *J. Org. Chem.* **1959**, *24*, 1051-1056.

[10] J. Muzart, *Chem. Rev.* **1992**, *92*, 113-140.

[11] a) X. Yang, L. T. Roling, M. Vara, A. O. Elnabawy, M. Zhao, Z. D. Hood, S. Bao, M. Mavrikakis, Y. Xia, *Nano Lett.* **2016**, *16*, 6644-6649; b) C. J. Serpell, J. Cookson, D. Ozkaya, P. D. Beer, *Nat. Chem.* **2011**, *3*, 478-483; c) X. Huang, Z. Zhao, L. Cao, Y. Chen, E. Zhu, Z. Lin, M. Li, A. Yan, A. Zettl, Y. M. Wang, *Science* **2015**, *348*, 1230-1234.

[12] a) G. J. Hutchings, *Chem. Commun.* **2008**, 1148-1164; b) J. A. Lopez-Sanchez, N. Dimitratos, N. Glanville, L. Kesavan, C. Hammond, J. K. Edwards, A. F. Carley, C. J. Kiely, G. J. Hutchings, *App. Catal. A* **2011**, *391*, 400-406.

[13] a) T. A. Silva, E. Teixeira-Neto, N. López, L. M. Rossi, *Sci. Rep.* **2014**, *4*, 5766; b) E. M. de Moura, M. A. Garcia, R. V. Gonçalves, P. K. Kiyohara, R. F. Jardim, L. M. Rossi, *RSC Adv.* **2015**, *5*, 15035-15041.

[14] a) Y.-M. Wang, S. L. Buchwald, *J. Am. Chem. Soc.* **2016**, *138*, 5024-5027; b) C. Weatherly, J. M. Alderson, J. F. Berry, J. E. Hein, J. M. Schomaker, *Organometallics* **2017**, *36*, 1649-1661.

[15] a) S. Karanjit, A. Jinasan, E. Samsook, R. N. Dhital, K. Motomiya, Y. Sato, K. Tohji, H. Sakurai, *Chem. Commun.* **2015**, *51*, 12724-12727; b) C. Shen, Z. Wei, H. Jiao, X. F. Wu, *Chem-Eur J* **2017**, *23*, 13369-13378.

[16] a) J. W. Fyfe, A. J. Watson, *Synlett* **2015**, *26*, 1139-1144; b) M. Marigo, P. Melchiorre, *ChemCatChem* **2010**, *2*, 621-623.

[17] a) C. Parmeggiani, C. Matassini, F. Cardona, *Green Chem.* **2017**, *19*, 2030-2050; b) T. Mallat, A. Baiker, *Chem. Rev.* **2004**, *104*, 3037-3058.

[18] C. M. Olmos, L. E. Chinchilla, A. Villa, J. J. Delgado, H. Pan, A. B. Hungría, G. Blanco, J. J. Calvino, L. Prati, X. Chen, *App. Catal. A* **2016**, *525*, 145-157.

[19] a) J. A. Gualteros, M. A. Garcia, A. G. da Silva, T. S. Rodrigues, E. G. Cândido, F. A. e Silva, F. C. Fonseca, J. Quiroz, D. C. de Oliveira, S. I. C. de Torresi, *J. Mater. Sci.* **2019**, *54*, 238-251; b) S. Oh, Y. K. Kim, C. H. Jung, W. H. Doh, J. Y. Park, *Chem. Commun.* **2018**, *54*, 8139-8282.

[20] D. Nepak, D. Srinivas, *RSC Adv.* **2015**, *5*, 47740-47748.

[21] L. Wang, H. Guo, X. Chen, Q. Chen, X. Wei, Y. Dinga, B. Zhua, *Catal. Sci. Technol.* **2015**, *5*, 3340-3351.

[22] P. J. Miedziak, Q. He, J. K. Edwards, S. H. Taylor, D. W. Knight, B. Tarbit, C. J. Kiely, G. J. Hutchings, *Catal. Today* **2011**, *163*, 47-54.

[23] S. Tauster, *Acc. Chem. Res.* **1987**, *20*, 389-394.

[24] P. Lu, X. Hu, Y. Li, M. Zhang, X. Liu, Y. He, F. Dong, M. Fu, Z. Zhang, *RSC Adv.* **2018**, *8*, 6315-6325.

[25] G. Blaise, C. Le Gressus, *AIP Adv.* **2018**, *8*, 095228.

[26] P. Ptáček, E. Bartoníčková, J. Švec, T. Opravil, F. Šoukal, F. Frajkorová, *Ceram. Int.* **2015**, *41*, 115-126.

[27] a) M. A. Alavi, A. Morsali, *Ultrason. Sonochem.* **2010**, *17*, 132-138; b) B. E. ScHrrrz, W. B. WHtrE, *Am. Mineral.* **1977**, *62*, 36-50; c) B. Sreedhar, M. Sulochana, C. S. Vani, D. K. Devi, N. S. Naidu, *Eur. J. Org. Chem.* **2014**, *3*, 234-239.

[28] a) J. Xu, T. White, P. Li, C. He, J. Yu, W. Yuan, Y.-F. Han, *J. Am. Chem. Soc.* **2010**, *132*, 10398-10406; b) J. K. Edwards, A. F. Carley, A. A. Herzing, C. J. Kiely, G. J. Hutchings, *Faraday Discuss.* **2008**, *138*, 225-239; c) Y. Mizukoshi, K. Sato, T. J. Konno, N. Masahashi, *Appl. Catal., B* **2010**, *94*, 248-253; d) T. Pasini, M. Piccinini, M. Blosi, R. Bonelli, S. Albonetti, N. Dimitratos, J. A. Lopez-Sanchez, M. Sankar, Q. He, C. J. Kiely, *Green Chem.* **2011**, *13*, 2091-2099; e) Q. Wang, X. Cui, W. Guan, X. Zhang, C. Liu, T. Xue, H. Wang, W. Zheng, *Microchim. Acta* **2014**, *181*, 373-380.

[29] C.-H. Cui, J.-W. Yu, H.-H. Li, M.-R. Gao, H.-W. Liang, S.-H. Yu, *ACS nano* **2011**, *5*, 4211-4218.

[30] a) V. Rico-Pérez, E. Aneggi, A. Trovarelli, *Catalysts* **2017**, *7*, 28; b) M. Ghelamallah, S. Kacimi, P. Granger, *Arab. J. Geosci.* **2018**, *11*, 221.

[31] I. A. Pašti, N. M. Gavrilov, S. V. Mentus, *Adv. Phys. Chem.* **2011**, *2011*.

[32] M. G. Sandoval, R. Luna, G. Brizuela, A. O. Pereira, C. Miranda, P. Jasen, *J. Phys. Chem. C* **2017**, *121*, 8613-8622.

[33] Y.-H. Ke, X.-X. Qin, C.-L. Liu, R.-Z. Yang, W.-S. Dong, *Catal. Sci. Technol.* **2014**, *4*, 3141-3150.

[34] Z.-L. Wang, J.-M. Yan, H.-L. Wang, Y. Ping, Q. Jiang, *J. Mater. Chem. A* **2013**, *1*, 12721-12725.

[35] T. C. Taucher, I. Hehn, O. T. Hofmann, M. Zharnikov, E. Zojer, *J. Phys. Chem. C* **2016**, *120*, 3428-3437.

[36] S. Dutta, C. Ray, S. Mallick, S. Sarkar, A. Roy, T. Pal, *RSC Adv.* **2015**, *5*, 51690-51700.

[37] M. Nerantzaki, M. Filippousi, G. Van Tendeloo, Z. Terzopoulou, D. Bikiaris, O. Goudouri, R. Detsch, A. Grüenewald, A. Boccaccini, *Express Polym. Lett.* **2015**, *9*, 773-789.

[38] Y. Wang, M. K. Bayazit, S. J. Moniz, Q. Ruan, C. C. Lau, N. Martsinovich, J. Tang, *Energ. Environ. Sci.* **2017**, *10*, 1643-1651.

[39] A. Shchukarev, D. Korolkov, *Open Chem.* **2004**, *2*, 347-362.

[40] J. Sun, X. Tong, Z. Liu, S. Liao, X. Zhuang, S. Xue, *Catal. Commun.* **2016**, *85*, 70-74.

[41] L. V. Candioti, M. M. De Zan, M. S. Camara, H. C. Goicoechea, *Talanta* **2014**, *124*, 123-138.

[42] D. Nepak, D. Srinivas, *RSC Advances* **2015**, *5*, 47740-47748.

[43] S. Sarina, H. Zhu, E. Jaatinen, Q. Xiao, H. Liu, J. Jia, C. Chen, J. Zhao, *J. Am. Chem. Soc.* **2013**, *135*, 5793-5801.

[44] W. Tang, G. Henkelman, *J. Chem. Phys.* **2009**, *130*, 194504.

[45] A. Savara, C. E. Chan-Thaw, J. E. Sutton, D. Wang, L. Prati, A. Villa, *ChemCatChem* **2017**, *9*, 253-257.

10.1002/cctc.201900512

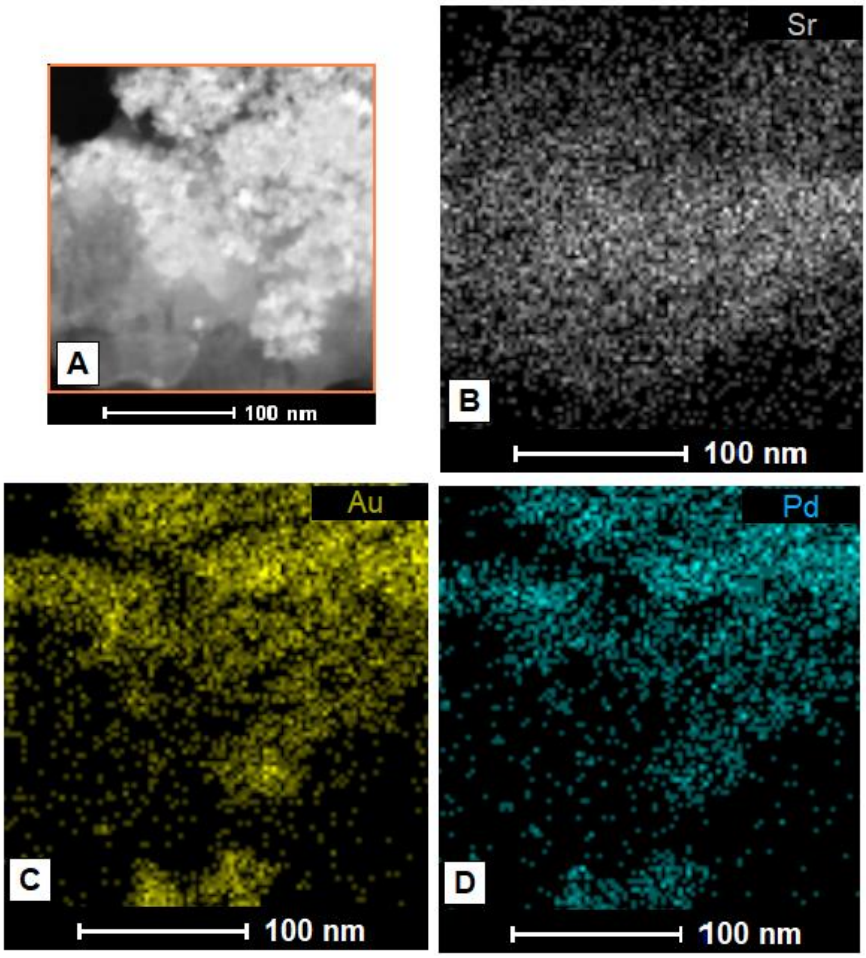

Fig. 1 The morphology of the as-prepared catalyst in the spectrum image scanning (A), and the STEM-EDS elemental map images of Sr, Au, Pd, and (B, C, D, respectively).

10.1002/cctc.201900512

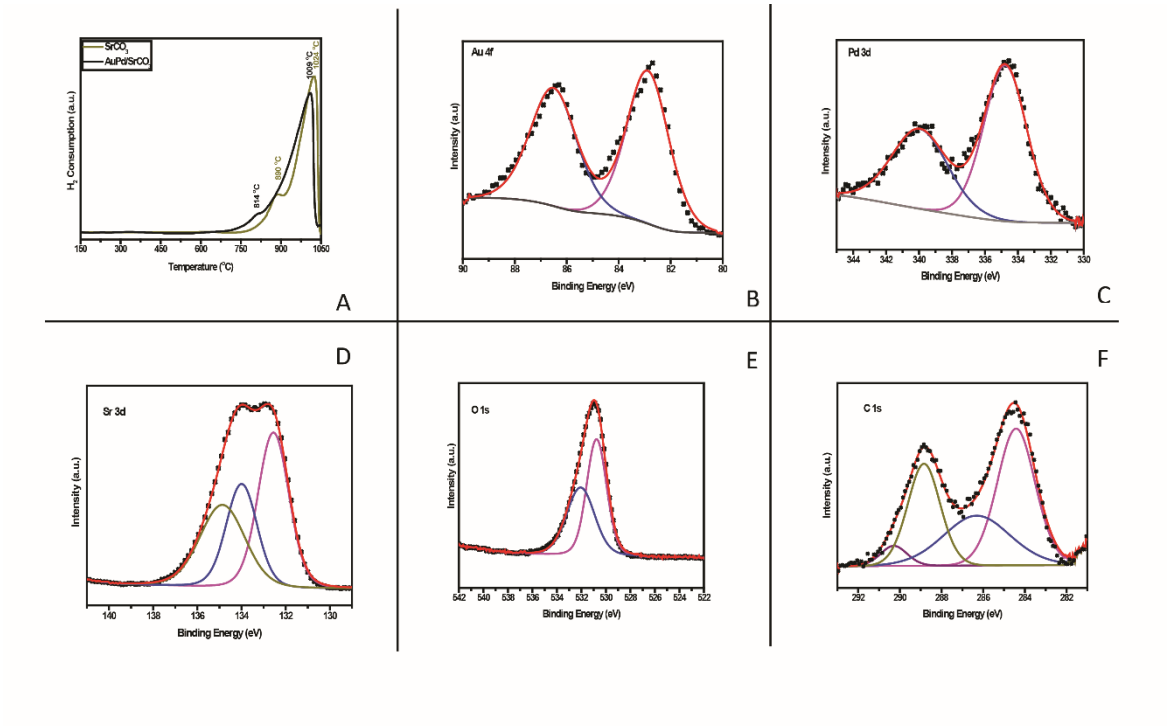

Fig. 2. (A) H_2-TPR profiles of $SrCO_3$ and Au-Pd/$SrCO_3$ catalyst. XPS spectra of (B) Au 4f, (C) Pd 3d, (D), Sr 3d, (E) O 1s, (F) C1s levels. The red line represents the fitted spectrum, and the black dots are the background.

10.1002/cctc.201900512

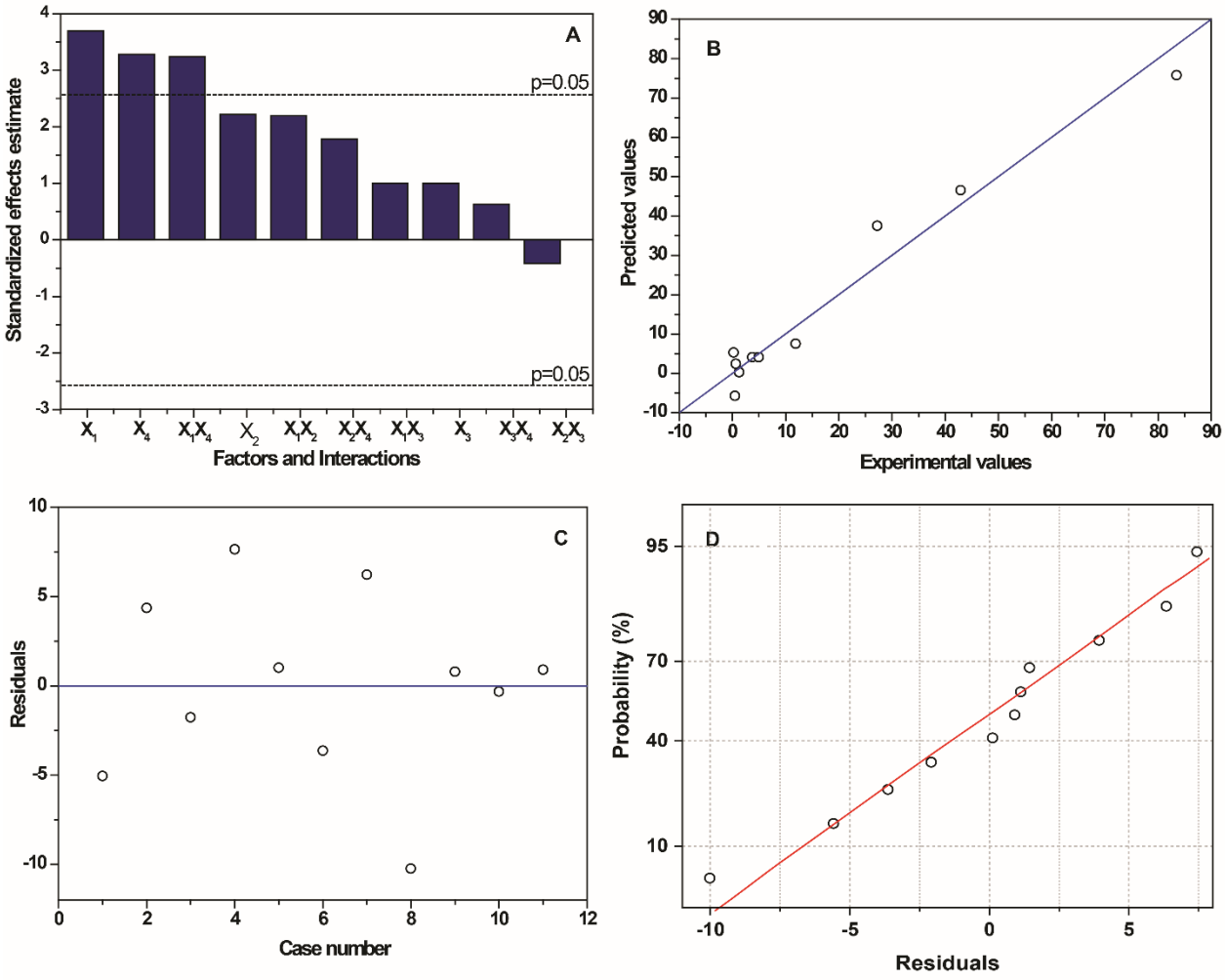

Fig. 3 (A) Pareto chart for the experimental design on benzyl benzoate yield (the horizontal dashed line, corresponding to a significance level of p = 0.05, indicates the significance of temperature, Au:Pd molar ratio, and the interaction between them for benzyl benzoate yield; the symbols are presented in Table 1; X_iX_j stands for the interaction between i and j factors). (B) Predicted *versus* experimental values for the benzyl benzoate yields (the values were predicted by the quadratic model from Equation 1). (C) Residuals of the quadratic model *versus* the case numbers. (D) Normal probability plot for the residuals from the quadratic model.

10.1002/cctc.201900512

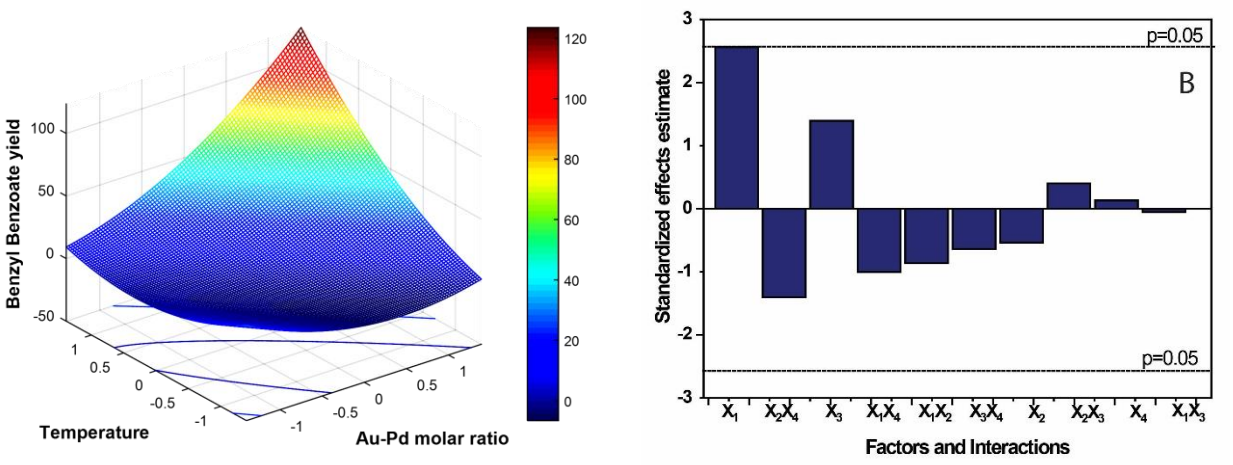

Fig. 4 (A) Response surface obtained from the quadratic model for benzyl benzoate yield. (B) Pareto chart for the experimental design on benzaldehyde yield (the horizontal dashed line corresponding to a significance level of $p = 0.05$ indicates the marginal significance of the Au:Pd molar ratio for benzaldehyde yield, the symbols are presented in Table 1; X_iX_j stands for the interaction between i and j factors).

10.1002/cctc.201900512

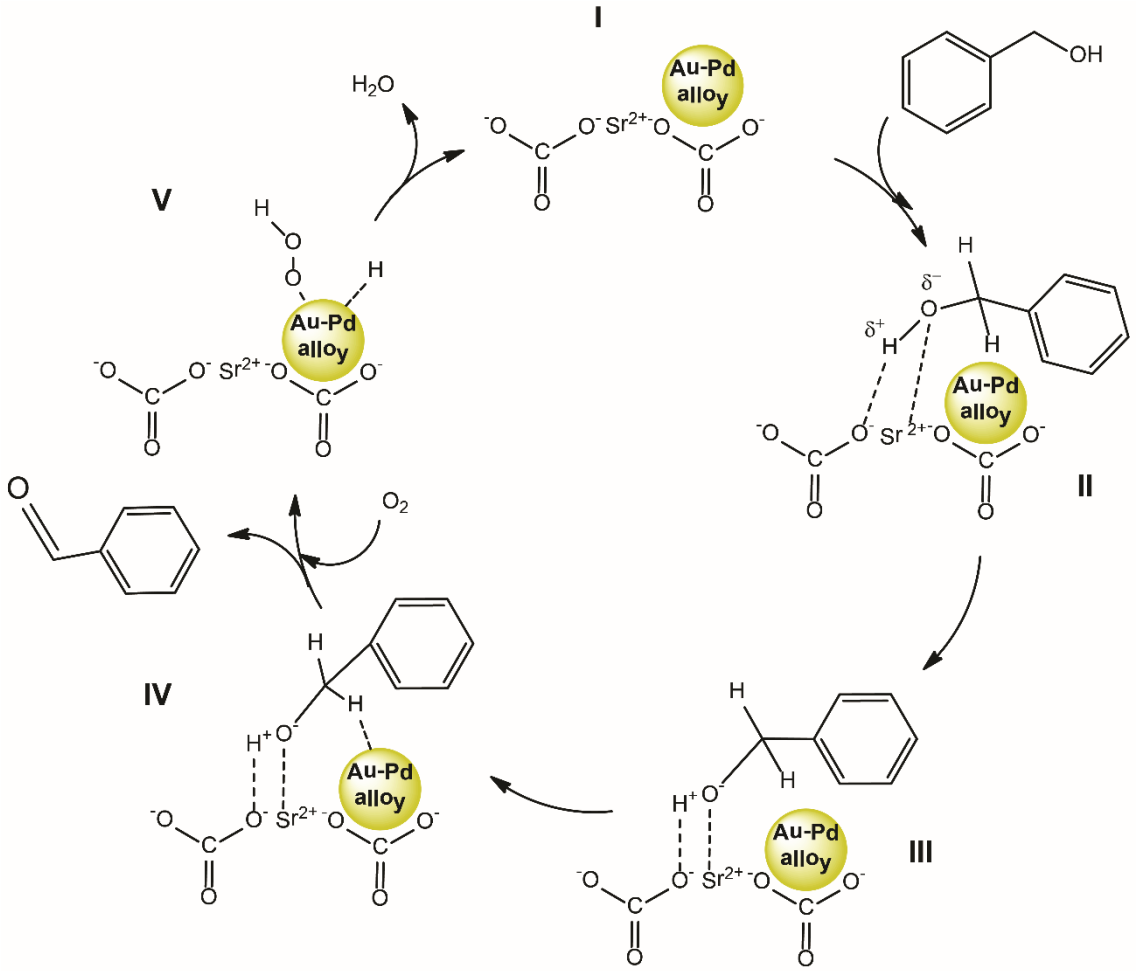

Fig. 5 Possible reaction pathway for the solvent-free oxidation of benzyl alcohol over Au–Pd/$SrCO_3$ catalyst for benzaldehyde formation.

10.1002/cctc.201900512

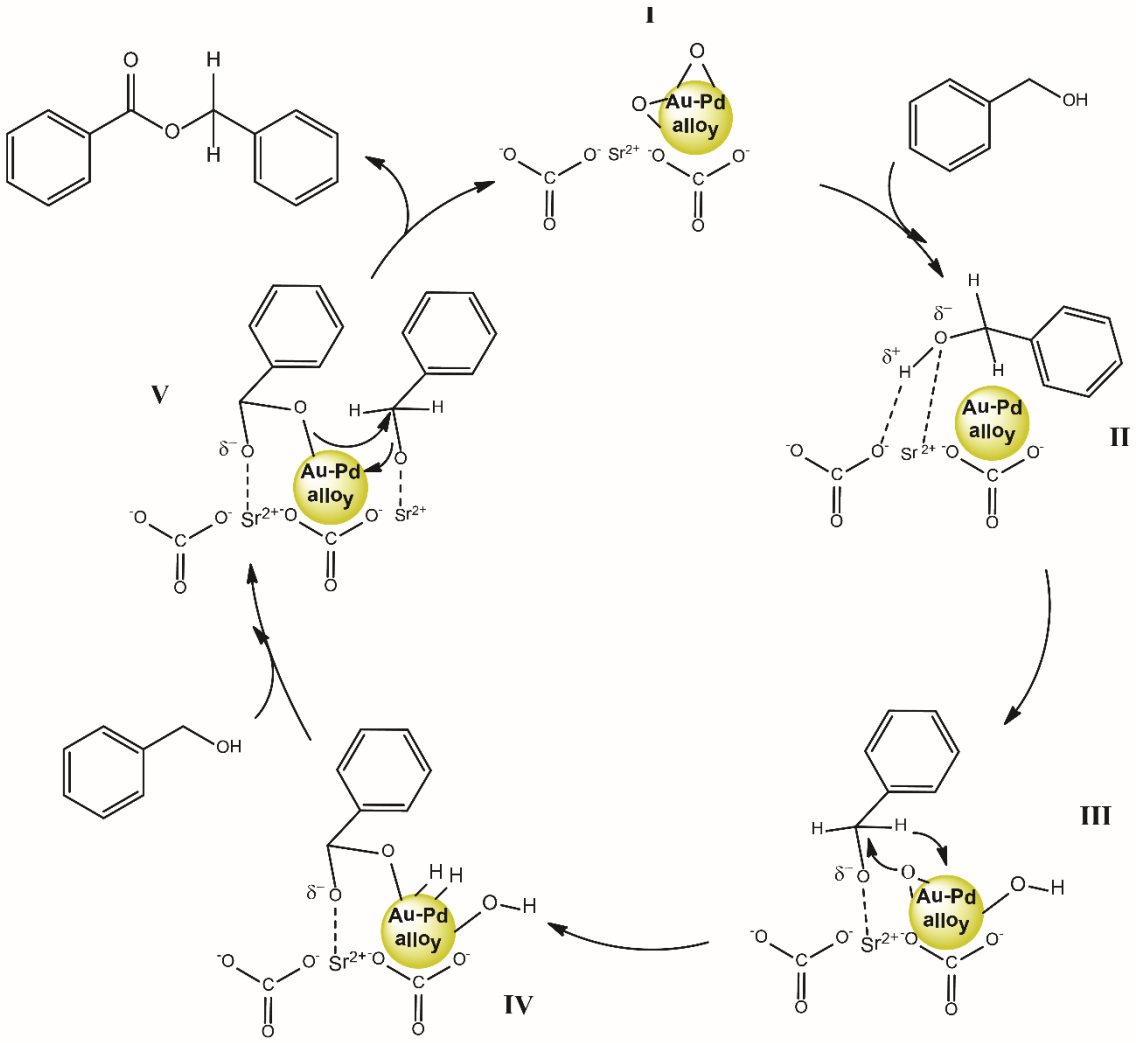

Fig. 6 Possible reaction pathway for the solvent-free oxidation of benzyl alcohol over Au–Pd/$SrCO_3$ catalyst for benzyl benzoate formation.

10.1002/cctc.201900512

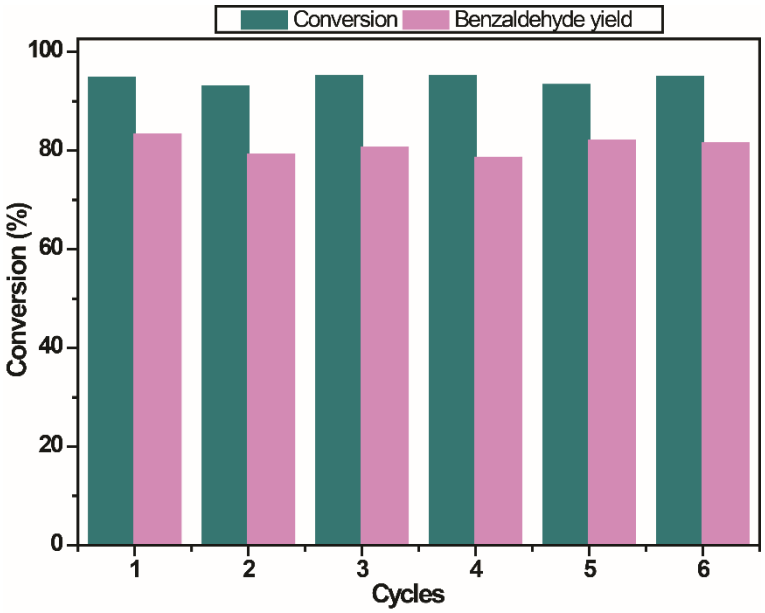

Fig. 7 Recycling tests for the Au-Pd/$SrCO_3$ catalyst in benzyl alcohol oxidation reactions under optimized conditions.

10.1002/cctc.201900512

Table 1. Full 2^4 factorial design for the screening of the temperature, reaction time, pressure and Au:Pd molar ratio on the benzyl benzoate and benzaldehyde yields.

		Factor levels				
Variables	**Symbols**	$-\sqrt{2}$	**-1**	**0**	**+1**	$+\sqrt{2}$
Au:Pd molar ratio	X_1	1:0*	1:0.1	1:0.8	1:1.5	1:1.6*
Pressure (bar)	X_2	-	1	-	5	
Reaction time (h)	X_3	-	0.5	-	2.5	-
Temperature (°C)	X_4	71.3	80	100	120	128,7

*the real codes of these variables are -1.14 and +1.14

Table 2. Lattice parameters, unit cell volume, site occupancy and atomic positions obtained from Rietveld refinements of Au-Pd/$SrCO_3$ catalyst.

Atoms	**Wyckoff**	**Site**	***x***	***y***	***z***	**Occupancy**
Sr1	4c	.m.	0.25000	0.41619(4)	0.75678(7)	1
C1	4c	.m.	0.25000	0.75873(4)	-0.08547(7)	1
O1	4c	.m.	0.25000	0.91118(5)	-0.09501(9)	1
O2	8d	1	0.46785(6)	0.68183(3)	-0.08610(6)	1

[Monophasic for $SrCO_3$; Pmcn (62) – Orthorhombic (a=5.0923(2) Å; b=8.3893(8), c=6.0100(9) Å, α=90º, β=90º, γ=90º; V=256.75(5) $Å^3$ Z=4; a/b=0.6070, b/c=1.3959, c/a=1.1802; R_p=0.205%, R_{wp}=0.255%; R_{exp}=0.072%; χ^2= 12.302 and GoF=3.507]

10.1002/cctc.201900512

Table 3. Full 2^4 factorial design and responses for benzyl benzoate and benzaldehyde yields.

Experiments	Variables*				Benzaldehyde yield (%)	Benzyl benzoate yield (%)
	X_1	X_2	X_3	X_4		
1	-1	-1	-1	-1	2.60	0.03
2	+1	-1	-1	-1	21.00	0.40
3	-1	+1	-1	-1	1.28	0.62
4	+1	+1	-1	-1	27.91	1.18
5	-1	-1	+1	-1	5.87	0.09
6	+1	-1	+1	-1	48.38	0.77
7	-1	+1	+1	-1	9.98	0.23
8	+1	+1	+1	-1	76.22	11.89
9	-1	-1	-1	+1	2.75	0.64
10	+1	-1	-1	+1	63.23	1.50
11	-1	+1	-1	+1	6.43	0.31
12	+1	+1	-1	+1	13.61	76.94
13	-1	-1	+1	+1	25.92	0.54
14	+1	-1	+1	+1	52.31	42.25
15	-1	+1	+1	+1	33.57	0.67
16	+1	+1	+1	+1	6.98	83.47

*According to descriptions of Table 1. The benzyl alcohol conversion and the products selectivity shown in Table S1 were used to calculate benzaldehyde and benzyl benzoate yield by Equation 3.

10.1002/cctc.201900512

Table 4. Additional data for the central composite design and responses for benzyl benzoate yields obtained for each experiment. Pressure and reaction time factors were maintained at 5 bar and 2.5 h, respectively.

Experiments	**Variables***		**Benzyl benzoate yield (%)**
	X_1	**X_4**	
17	-1.14	0	0.49
18	+1.14	0	27.24
19	0	$-\sqrt{2}$	1.27
20	0	$+\sqrt{2}$	42.90
21	0	0	4.88
22	0	0	3.76
23	0	0	4.98

*According to descriptions of Table 1.

10.1002/cctc.201900512

Table 5. ANOVA table for the benzyl benzoate yields predicted by the quadratic model.

Variation source	**Sum of Squares (SS)**	**Degrees of freedom (DF)**	**Mean Squares (MS)**	***F* value**	***p*-value**
X_1	2141.645	1	2141.645	4667.928	0.000214
X_1^2	558.724	1	558.724	1217.795	0.000820
X_4	2364.229	1	2364.229	5153.070	0.000194
X_4^2	271.325	1	271.325	591.380	0.001687
X_1X_4	1265.225	1	1265.225	2757.683	0.000362
Lack of fit	264.704	3	88.235	192.316	0.005177
Pure error	0.918	2	0.459		
Total	6752.151	10			

10.1002/cctc.201900512

Table of contents

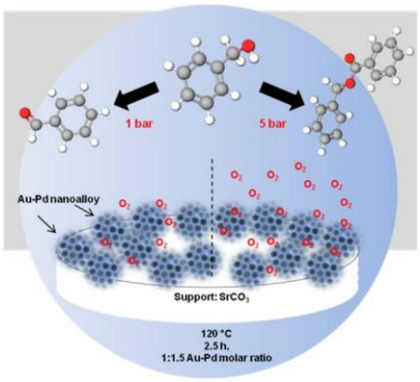

We have proposed a catalyst comprised of an Au-Pd nanoalloy supported on $SrCO_3$ that can modify the benzyl alcohol selectivity by just changing the pressure of the system. At 5 bar, the chemoselectivity was demonstrated to be for the benzyl benzoate, and at 1 bar, high yields of benzaldehyde were obtained. We were able to prepare a catalyst that is a real selectivity-switchable material.